Kinetic and Thermodynamic Studies on the Adsorption of Zn^{2+} onto Chitosan-aluminium Oxide Composite Material

Zhiguang Ma, Na Di, Fang Zhang, Peipei Gu, Suwen Liu & Pan Liu (Corresponding author)

College of Chemistry and Environmental Science, Hebei University

Baoding 071002, China

Tel.: 86-312-507-9795   E-mail: hbumzg@163.com

Abstract

This study presents kinetic and thermodynamic studies on the adsorption of Zn^{2+} onto chitosan-aluminium oxide composite material. The adsorption of Zn^{2+} onto chitosan-aluminium oxide composite material was found to follow pseudo-second-order kinetic model and the apparent adsorption activation energy (Ea) was measured to be 37.20kJ/mol. Adsorption was mainly chemical adsorption. Thermodynamic data supported Langmuir adsorption model and the enthalpy of adsorption (ΔH^{θ}) and the entropy of adsorption (ΔS^{θ}) were found to be 17.81kJ/mol and 109.77J/(mol·K), respectively. The adsorption Gibbs free energy (ΔG^{θ}) decreased with the increase of temperature.

Keywords: Chitosan, Composite material, Adsorption, Kinetic, Thermodynamic

1. Instruction

Chitosan is a linear polysaccharide composed of randomly distributed β-(1-4)-linked D-glucosamine and N-acetyl-D-glucosamine. It has high adsorption capacity for a variety of heavy metals including zinc, copper, and mercury (Majeti, N V., & Ravi, K. 2000; Chu, K H. 2002; Burke, A., Yilmaz, E., & Hasirci, N. 2002; Dhakal, R P., Inoue, K., & Yoshizuka, K. 2005). Furthermore, chitosan can be easily synthesized through chitin deacetylation with low cost. These two characteristics make chitosan an excellent candidate for manufacturing commercial adsorbent for wastewater treatment and heavy metal enrichment and recycling (Mayumi, M., Hiroaki, M., Shoichiro, Y., & Nobuharu, Y J. 2004; Veera, M. B., Drishnaiah, A., Jonathan, L. T., & Edgar, D S. 2003). As an organic compound, chitosan has poor sulfuric acid resistance and weak mechanical strength, thus limiting its commercial applications. In addition, the presence of large amount of hydrogen bonding within chitosan could decrease its adsorption capacity. Aiming to overcome these limitations, it has been demonstrated that synthesis of chitosan-inorganic composite material can be a promising approach for the design of new chitosan adsorbents. For example, Xie et al (Xie, G. Y., & Du, C Q. 2009) prepared the chitosan-aluminium oxide composite material using chitosan and isopropanol aluminum and found that the adsorption capacity of such composite towards copper ions and mercury ions had been greatly improved.

In this study, we focus on a better understanding towards the fundamental aspects of the adsorption of heavy metal such as zinc onto chitosan-aluminium oxide composite and present a thorough kinetic and thermodynamic investigation of the adsorption process. We hope our results help to provide valuable insights for a better design of chitosan-inorganic composite materials.

2. Experimental

2.1 reagents

Chitosan (>90%, Zhejiang Golden-shell Biochemical Co., Ltd. China), Isopropanol aluminum (>99.5%,Sinopharm Chemical Reagent Co., Ltd. China), $ZnSO_4·6H_2O$(>99.5%,Sinopharm Chemical Reagent Co., Ltd. China), EDTA, Ammonium chloride, Ammonia water, Eriochrome balck T, Toluene, Ethanol, All reagents used were of analytical reagent grade.

2.2 Experimental methods

Chitosan-aluminum oxide composite material was prepared according to the procedure described in previous study (Xie, G. Y., & Du, C Q. 2009). Briefly, 3g of isopropanol aluminum was added into 100ml of toluene in a three-neck bottle equipped with reflux condenser. The mixture was kept at 50 ℃ under nitrogen protection and stirring for 30min. Then 10g chitosan was added into the mixture and the mixture was kept at 112 ℃ for 5h. The crude product first went through leaching and washing with toluene, ethanol, and distilled water, and then dried at 80 ℃ in an oven.

Adsorption experiments were carried out in a flask placed in a water bath oscillator. 0.5000g composite material was added into $ZnSO_4$ solution to carry the adsorption study. The oscillator oscillated at 130r/min. EDTA titration was used to quantify the amount of Zn^{2+} onto the composite material. Adsorption was calculated by according to equation (1)

$$Q = (C_0\text{-}C) \times V / m \tag{1}$$

Where Q is adsorption capacity, C_0 and C are the initial concentration and the final concentration of Zn^{2+}, V is the solution volume, and m is the adsorbent mass.

For each adsorption experiment, the average of three replicates was recorded.

3. Result and discussion

3.1 Kinetic studies on the adsorption of Zn^{2+} onto chitosan-aluminum oxide composite material

Fig. 1 shows the adsorption kinetic curve of Zn^{2+} from a $0.04mol.L^{-1}$ solution onto the chitosan-aluminum oxide composite material at different temperatures. The results demonstrated that the composite material had better adsorption properties compared with previous results. This adsorption procedure was generally consistent with the three-step adsorption behavior usually observed from porous adsorbents (Huang, Y. R., Li, Z. J., Wang, H. F., Miao, Z .C., & Liu, J. G. 2009). Initially, the adsorption rate was fast, and then decreased over time, after about 480 minutes later, the adsorption reached equilibrium. This adsorption behavior was attributed to that: at the beginning, the adsorption of Zn^{2+} onto composite material mainly occurred on the external surface of composite material and the adsorption rate was rapid. The concentration of Zn^{2+} then began to decrease over time as adsorption progressed. Meanwhile, adsorbed zinc ions diffused inward into the composite material through the micropore, and the resistance of diffusion increased. Adsorption rate was mainly controlled by diffusion at this stage, so the rate of adsorption was becoming small. At the final stage, the adsorption mainly occurred on the inner surface of adsorbent while the concentration of zinc in the solution became smaller, and the adsorption reached equilibrium at the last stage. Temperature had a positive effect on the adsorption. When the temperature increased, the rate of adsorption increased correspondingly since the percentage of activated molecules increased.

Pseudo second order kinetics model was used to fit the kinetic data. This model is based on assumption of that: the rate of adsorption is determined by the square of the number of vacancies (Sun, X. L., Zeng, Q. X., & Feng, C. G. 2009). The formula is:

$$dQ_t/dt = k\ (Q_{eq}\text{-}Q_t)^2 \tag{2}$$

Integration of equation (2) under boundary conditions resulted in equation (3)

$$t/Q_t = t/Q_{eq} +1/kQ_{eq}^2 \tag{3}$$

where Q_t $(mmol \cdot g^{-1})$ is the absorption amount at time t (minute); and Q_{eq} $(mmol \cdot g^{-1})$ is the absorption amount at equilibrium; k is the adsorption rate constant $(g.mmol^{-1}.min^{-1})$.

If adsorption procedure conforms to pseudo-second-order equation, t / Q_t and t could have a linear relationship. Fitting the data in fig. 1 by the pseudo-second-order-kinetic equation resulted in a straight line as shown in fig 2. Correlation coefficients R^2 are all better than 0.999, and speed constant k and the enhancement of initial concentration of solution also have good relevance. Therefore, the pseudo-second-order equation is a suitable model to describe this adsorption procedure. Because the pseudo-second-order equation is usually used to describe chemical adsorption process, we hypothesize that the adsorption procedure in our study was primarily chemical adsorption (Ho, Y. S. 2006). We can also obtain the values of Q_{eq} and k from the slope and intercept, as listed in Table 1.

Temperature study (lnk versus 1/T) showed a R^2 value of 0.9967. This indicated that the relationship between temperature and the rate of absorption obeyed the Arrhenius equation. The temperature had significant effect on the rate constant k. When the temperature increased, solute movement became faster and the collision frequency between solute and absorbent surface became higher, thus making adsorption capacity bigger. It is well known that physical adsorption is a reversible dynamic procedure, and it can reach equilibrium quickly. The activation energy for physical adsorption procedure is usually no more than $4.2kJ\ mol^{-1}$ because physical adsorption procedure only requires weak force. In contrast, chemical adsorption needs high activation energy (Aksu, Z. 2002). According to the Arrhenius equation we obtained Ea was $37.20kJmol^{-1}$. This further proved our previous hypothesis that the adsorption procedure was chemical adsorption.

3.2 Thermodynamic studies on the adsorption of Zn^{2+} onto chitosan-aluminium oxide composite material

Data in Table 2 indicated that the adsorption capacity of Zn^{2+} on the composite material increased with the increase of the initial concentration of Zn^{2+} in solution, and then it reached a maximum value. This was due to that the

amount of composite material was at a fixed value and thus the number of adsorption sites was at a fixed too. At the beginning of the adsorption, the composite materials could provide enough sites, thus the adsorption capacity of composite materials was high (Cheng, Y. N., & Ding, Y. C. 2009); however, the active sites became insufficient when the initial concentration of Zn^{2+} was high and the adsorption sites could be saturated under such situation. That's why when the concentration of Zn^{2+} became $0.09 mol.L^{-1}$ or higher, the adsorption capacity of Zn^{2+} on the composite materials became constant.

Form table 2, we can further explore the relation between different initial concentration and temperature and adsorption amount. Date in table 2 was fitted according to two different models, Freundlich adsorption model and Langmuir adsorption model. The expressions of the two models are listed below.

$$\text{Freundlich adsorption model to meet: } lgQ_m = blgC_m + lga \qquad (4)$$

$$\text{Langmuir adsorption model to meet: } C_{eq}/Q_{eq} = C_{eq}/Q_m + 1/K_L Q_m \qquad (5)$$

Where, Q_m is the saturated adsorption capacity ($mmol.g^{-1}$); C_{eq} and Q_{eq} are the equilibrium concentration of metal ions ($mmol.L^{-1}$) and the adsorption capacity ($mmol.g^{-1}$), respectively, K_L ($L.mmo^{-1}$) is the Langmuir constant ($L.mmo^{-1}$).

Form the table 3, we can see that all the correlation coefficient of Langmuir equation were better than 0.999. The adsorption of Zn^{2+} onto the composite material was consistent with the Langmuir model, in stead of Freundlich model. Fig 3 shows Langmuir adsorption model for Zn^{2+} adsorption. This suggested that the adsorption procedure was consistent with a monolayer adsorption model, meaning one adsorption site only absorbs one Zn^{2+} ion and when all of the adsorption sites were occupied, the adsorption reached dynamic equilibrium (Chen, S. W., Shi, W. J., Song, W., Qin, Q., Zhang, Y. Z., & Gao, J. C. 2009).

From table 4, we can see that: When the temperature increases, the saturated adsorption capacity of composite materials and Langmuir equilibrium constants become greater, so it is clearly that the absorption is endothermic.

The relationship between K_L and T can be obtained from the Van't Hoff equation (Atia, A., Donia, A. M., & El-Boraey, H. A. 2006).

$$lnK_L = -\Delta H^o/RT + \Delta S^o/R \qquad (6)$$

Where ΔH^o ($J.mol^{-1}$) and ΔS^o ($J.mol^{-1}.K^{-1}$) are the enthalpy of adsorption and the entropy of adsorption, respectively, R is perfect gas constant, T (K) is temperature. lnK_L had a linear relationship with $1/T$ with a R^2 value of 0.9148. The slope and intercept are $-\Delta H^o/R$ and $\Delta S^o/R$, respectively, and ΔH^o and ΔS^o were determined to be 17.81 $kJ.mol^{-1}$ and $109.77 J.mol^{-1}.K^{-1}$. ΔH^o was positive, and it indicated that the adsorption of Zn^{2+} onto compound materials was endothermic, and this also explained why the rate of adsorption of Zn^{2+} onto compound materials increased with the increase of temperature. ΔS^o was also positive, and this meant an irregular increase of the randomness at the composite material -solution interface during adsorption procedure.

The results of ΔG^o were listed in Table 5. Gibbs free energy (ΔG^θ) was negative at all four temperatures. ΔG^θ decreased with the increase of temperature. It suggested that the adsorption of Zn^{2+} on the composite material was a spontaneous procedure, the spontaneous degree become greater with the increase of temperature. Increasing temperature is beneficial to the adsorption procedure.

4. Conclusion

The adsorption kinetics of Zn^{2+} onto chitosan-aluminum oxide composite materials was found to follow the pseudo-second-order kinetic model. Adsorption procedure was mainly chemical adsorption, and the apparent adsorption activation energy was measured. Thermodynamic studies indicated that the adsorption procedure conformed to the Langmuir adsorption model and the adsorption satisfied monolayer adsorption theory. The adsorption thermodynamic parameters were obtained. This adsorption reaction was found to be exothermic.

References

Aksu, Z. (2002). Determination of equilibrium kinetic and thermodynamic parameters of the batch biosorption of nickel(II)ions onto Chlorella vulgaris. *Process Biochemistry*, 38, 89-99.

Atia, A., Donia, A. M., & El-Boraey, H. A. (2006). Adsorption of Ag(I) on glycidyl methacrylate/N,N′-methylene bis-acrylamide chelating resins with embedded iron oxide. *Separation and Purification Technology,* 48, 281-287.

Burke, A., Yilmaz, E., & Hasirci, N. (2002). Iron(III) ion removal from solution through adsorption on chitosan. *Journal of Applied Polymer Science*, 84, 1185-1192.

Chen, S. W., Shi, W. J., Song, W., Qin, Q., Zhang, Y. Z., & Gao, J. C. (2009). Kinetic and thermodynamic studies.on the adsorption of acid dyes onto chitosan-β-cyclodextrin polymer. *Journal of Functional Materials*, 40, 656-659.

Cheng, Y. N., & Ding, Y. C. (2009). Kinetics, Thermodynamics Study on the Adsorption of Husk to Cadmium Ions in Water, *Journal of Anhui Agriculture Science*, 37, 3190-3192.

Chu, K H. (2002). Removal of copper from aqueous solution by chitosan in prawn shell: adsorption equilibrium and kinetics. *Journal of Hazardous Materials*, 90, 77-95.

Dhakal, R P., Inoue, K., & Yoshizuka, K. (2005). Solvent Extraction of Some Metal Ions with Lipophilic Chitin and Chitosan. *Solvent Extraction and Ion Exchange*, 23, 529-543.

Ho, Y. S. (2006). Second-order kinetic model for the sorption of cadmium onto tree fern: A comparison of linear and non-linear methods. *Water Research*, 40, 119-125.

Huang, Y. R., Li, Z. J., Wang, H. F., Miao, Z .C., & Liu, J. G. (2009). Study on adsorption and kinetics of anion starch microspheres for Cr^{3+}. *Applied Chemical Industry*, 38, 1093-1097.

Majeti, N V., & Ravi, K. (2000). A review of chitin and chitosan applications. *Reactive and Functional Polymers,* 46, 1-27.

Mayumi, M., Hiroaki, M., Shoichiro, Y., & Nobuharu, Y J. (2004). Adsorption behavior of heavymetals on biomaterials. *Journal of agricultural and food chemistry*, 52, 5606-5611.

Sun, X. L., Zeng, Q. X., & Feng, C. G. (2009). Adsorption kinetics of chromium (Ⅵ) onto an anion exchange fiber containing polyamine. *Wuli Huaxue Xuebao*, 25, 1951-1957.

Veera, M. B., Drishnaiah, A., Jonathan, L. T., & Edgar, D S. (2003). Removal of hexavalent chromium from wastewater using a new composite chitosan bisorbent. *Environmental Science and Technology*, 37, 4449-4456.

Xie, G. Y., & Du, C Q. (2009). Preparation, characterization and adsorption for Cu^{2+} of chitosan-aluminium(III) oxide composite material. *Ion Exchange and Adsorption*, 25, 200-207.

Table 1. Adsorption dynamic parameters at different temperatures

T/K	$Q_{eq}/(mmol \cdot g^{-1})$	$k/(g \cdot mmol^{-1} \cdot min^{-1})$	R^2
298K	1.8372	0.01889	0.9992
308K	1.8549	0.03239	0.9999
318K	1.8591	0.04725	0.9999
328K	1.8754	0.07658	0.9999

Table 2. Influence of concentration on the adsorption capacity of Zn^{2+} onto the composite materials

C_o (mol/L)	298K		308k		318k		328k	
	C_{eq} (mmol/L)	Q_{eq} (mmol /g)	C_{eq} (mmol/L)	Q_{eq} (mmol /g)	C_{eq} (mmol/L)	Q_{eq} (mmol /g)	C_{eq} (mmol/L)	Q_{eq} (mmol /g)
0.04000	5.050	1.7475	4.1810	1.7910	3.7620	1.8119	3.1680	1.8416
0.05000	9.365	2.0317	7.6230	2.1189	6.6340	2.1683	5.2870	2.2357
0.06000	16.20	2.1900	13.860	2.3070	12.610	2.3695	10.690	2.4655
0.07000	24.24	2.2880	21.880	2.4060	20.790	2.4605	18.470	2.5765
0.08000	32.12	2.3941	30.040	2.4980	29.600	2.5200	27.130	2.6435
0.09000	42.42	2.3790	40.100	2.4950	38.710	2.5645	37.820	2.6090

Table 3. Freundlich and Langmuir equation

Temperature(K)	Freundlich equation	R^2	Langmuir equation	R^2
298k	$lgQ_{eq}=0.1461lgC_{eq}+0.1540$	0.9472	$C_{eq}/Q_{eq}=0.3966C_{eq}+0.9036$	0.9995
308k	$lgQ_{eq}=0.1440lgC_{eq}+0.1837$	0.9228	$C_{eq}/Q_{eq}=0.3784C_{eq}+0.7953$	0.9996
318k	$lgQ_{eq}=0.2175lgC_{eq}+0.1284$	0.9460	$C_{eq}/Q_{eq}=0.3746C_{eq}+0.6263$	0.9999
328k	$lgQ_{eq}=0.1328lgC_{eq}+0.1315$	0.8439	$C_{eq}/Q_{eq}=0.3681C_{eq}+0.4331$	0.9994

Table 4. Parameters and equations for Langmuir adsorption model

T/K	Langmuir equation	$Q_m/(mmol \cdot g^{-1})$	$K_L/(L \cdot mmol^{-1})$	R^2
298	$C_{eq}/Q_{eq}=0.3966C_{eq}+0.9036$	2.5215	0.4389	0.9995
308	$C_{eq}/Q_{eq}=0.3784C_{eq}+0.7953$	2.6430	0.4757	0.9996
318	$C_{eq}/Q_{eq}=0.3746C_{eq}+0.6263$	2.6699	0.5980	0.9999
328	$C_{eq}/Q_{eq}=0.3681C_{eq}+0.4331$	2.7169	0.8499	0.9994

Table 5. the results of ΔG^o at different temperatures

T/K	298K	308K	318K	328K
$\Delta G^o/(kJ \cdot mol^{-1})$	-14.90	-15.60	-17.10	-18.19
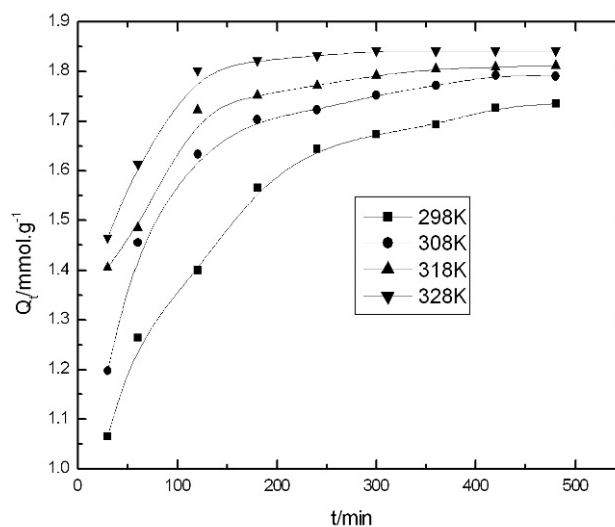
Figure 1. Adsorption rate of Zn^{2+} at different temperatures
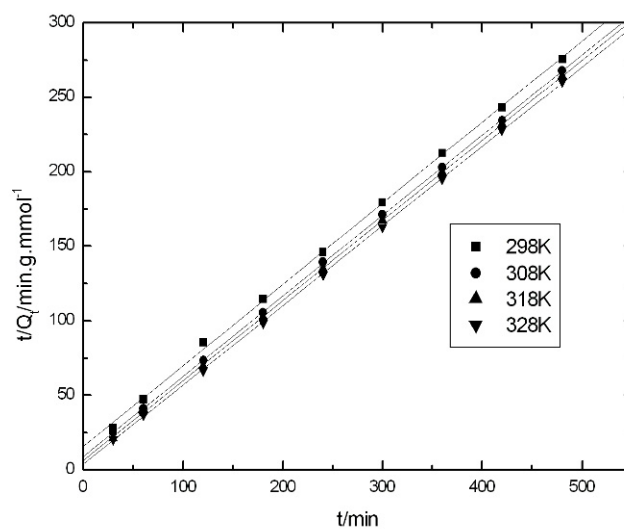
Figure 2. Pseudo second-order equation plots
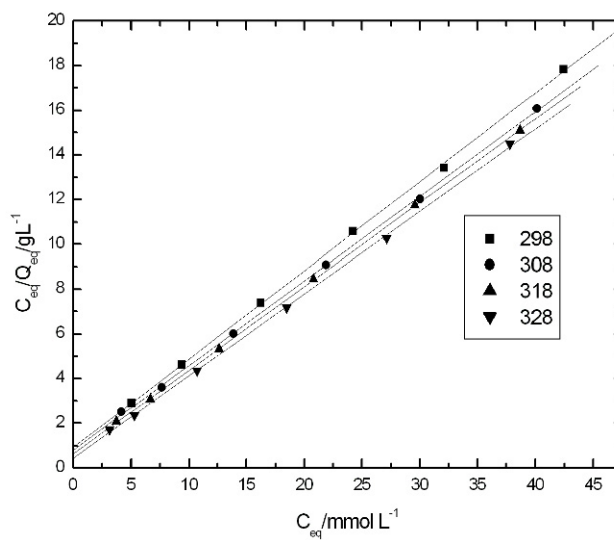
Figure 3. Fitting using Langmuir adsorption model for Zn^{2+} adsorption